



SOLAR PANEL LIFETIME DETECTION USING DEEP LEARNING NETWORK BASED ON TEMPERATURE AND HUMIDITY SENSORS

YINGHUA ZHENG* AND YUANYUAN ZHENG †

Abstract. Solar photovoltaic (PV) performance is reduced due to the increase in panel temperature. Solar PV panels must be kept at an ideal temperature to work at their peak and have the longest useful life possible. The current generation of temperature sensors has a slow response time, poor resolution, and poor accuracy. More precision, a larger dynamic range, and very high sample rates are all provided by fiber-optic sensors. This study develops a revolutionary deep learning-based method for predicting the lifespan of solar panels in order to maintain efficiency and maximise their usefulness. At first, the temperature and humidity (TH) data are collected from the solar photovoltaic panel using the fibre-optic sensor and Sensirion SHT15 sensor. The primary device of the solar PV panel lifetime detection system is Raspberry Pi which is used to store the data collected by different sensors. These data are transferred to cloud server using Raspberry Pi. Based on the gathered data the deep learning-based Bi-LSTM network is used to detect the panel lifetime using the threshold value. Furthermore, the GSM module will notify consumers if any alterations are made to the solar panel. The efficacy of the proposed model was assessed utilising the precise criteria, such as sensitivity, accuracy, and specificity. The proposed method's accuracy of 95.2% is higher than that of conventional DL networks. By using certain measures like specificity, sensitivity, and accuracy, the suggested Bi-LSTM improves on classic CNN and LSTM by 1.78% and expands the accuracy rate range by 4.20%. The proposed method's accuracy of 95.2% is higher than that of conventional DL networks. Compared to conventional CNN and LSTM, the suggested Bi-LSTM improves overall trend by 4.20% and 1.78%, respectively.

Key words: Solar photovoltaic panel, Deep learning, Lifetime detection, Fibre-optic sensor, Sensirion SHT15 sensor

1. Introduction. Solar energy is among the most widely used renewable energy sources and methods of selectively capturing solar energy can be used in residential settings. Due to technological advancements in this area and its environmental friendliness, solar energy has a promising future [1]. In addition to its year-round unavailability, solar energy is also extremely expensive and it is difficult to source PV cell components. These problems can be solved by developing an efficient system to store energy and manufacturing Solar pv cells that are inexpensive, efficient, and abundant. The relatively low quality at increased panel temperatures is one of the most major disadvantages of residential solar cells [2]. Monitor heat, radiation from the sun, shadows, panel propensity, orientation, dust, and maintenance are examples of external factors that have a negative impact on the efficiency of solar panels. Monocrystalline silicon solar cells can lose up to 0.045% efficiency when temperature rises by one degree between 15 and 60 [3,4]

Thermocouples, Resistance Temperature Detector (RTD) sensors, and thermal imaging cameras are commonly used to monitor the temperature of solar PV modules. In addition to these flaws, traditional approaches are also prone to self-heating, poor resolution, nonlinear response, and slow response times [5]. Due to their resistance to electromagnetic interference, fiber-optic sensors, which have high susceptibility, wide range, and high multiplexer capability, offer a possible alternative solution. Numerous investigations have focused on the functional abnormalities associated with solar panel [6]. In recent days several frameworks were introduced by the researchers primarily to increase the lifetime of solar panel with different sensor and various artificial intelligence approaches, some of those frameworks are studied briefly in this research.

In 2019, Chaibi et al. [7] examined the current-voltage (I-V) characteristics of Si-crystalline PV modules under non-standard irradiation and temperature conditions. Each equivalent circuit model's parameters were calculated using this procedure. Then, at various levels of temperature and irradiance, the I-V curves supplied by the manufacturers and the computed I-V characteristics are compared. It is possible to achieve error reductions

*Xinxiang Vocational and Technical College, Xinxiang, Henan, 453006, China (Corresponding author, YinghuaZheng6@126.com)

†Yongji Senior Technical School of Electric Machinery, Yongji, Shanxi, 044500, China. (YuanyuanZheng7@163.com)

of 53.93% and 21.04%, respectively. In 2019 Zaimi., et al., [8] presented two methods for calculating model-physical solar panel parameters using photovoltaic metrics. The first approach establishes a critical connection between series resistance, quality factor, and photovoltaic metrics, resulting in a transcendental equation. The second way of expressing series resistance is to create an analytical expression that is based on the quality factor and key point coordinates of the series. For both approaches, To represent parallel conductance, image current, and leakage current, q - factor and all other PV characteristics must be used. An outfit deep convolutional neural network (DNN) model for the automated detection of visual flaws such as glass breaking, burn marks, snail trails, and discolouration, failure mode on various PV modules was created by Venkatesh et al. in 2022 [9].

The existing methods used to monitor the temperature of PV modules are thermocouples, Resistance Temperature Detector (RTD) sensors, and thermal imaging cameras. There are several flaws to these traditional approaches, including poor precision, nonlinear response, poor resolution, slow response time, and self-heating [10, 11]. Due to their high sensitivity, wide range, and potential for multiplexing, fiber-optic sensors offer a promising substitute strategy. FBG sensors are widely used to measure temperature and strain in distributed environments [12]. The precision of the peak detection algorithms that enable the conversion of a registered signal into temperature/strain values heavily influences the performance of FBG-based sensors [13,14]. To prevent mutual interference between nearby FBGs, an array of FBGs is frequently sparsely inscribed on a length of fibre in the spatial and spectral domains. Thus, several processing techniques can be used because it is relatively easy to discern the locations and shapes of the peaks [15]. The main contributions of the research work are summarized as follows:

- The primary purpose of this research is to designed a novel Deep learning-based solar panel lifetime prediction for sustaining performance and maximizing the productive life of solar panels.
- Initially, two different sensors such as temperature sensor and humidity sensor have been used for collecting TH data of essential parameters continuously.
- These data are transferred to cloud server using Raspberry Pi. The deep learning-based Bi-LSTM network is used to detect the panel lifetime based on the obtain threshold value the alert message is send to the user.
- The efficacy of the proposed model was assessed using the specific metrics like specificity, sensitivity and accuracy.

The rest of this work is pre-arranged as follows: section-2 describes the literature survey on neonatal cry signal, section-3 enlightens the inclusive work of the proposed methodology, section-4 narrates the experimental fallouts and discussion and section-5 encloses with the conclusion.

2. Proposed Methodology. In this section, a novel Deep learning-based solar panel lifetime prediction for sustaining performance and maximizing the productive life of solar panels.

Initially, the temperature and humidity data are collected from the solar photovoltaic panel using the fibre-optic sensor and Sensirion SHT15 sensor. These data are transferred to cloud server using Raspberry Pi. Based on the gathered data the deep learning-based Bi-LSTM network is used to detect the panel lifetime using the threshold value. The schematic representation of the proposed methodology is shown in figure.2.1.

2.1. Sensors deployed. The temperature and humidity (TH) data are gathered from two sensors namely FBG and SHT15 sensors. In optical fibers, fibre Bragg gratings (FBGs) cause periodic fluctuations in refractive index. FBG sensors are precise and adaptable thermometers. There is a microstructure within an optical fiber's core called FBG that periodically modifies the refractive index of the underlying glass material. It is possible to create fibre Bragg gratings by exposing a single-mode core of fiber that is laterally to recurring patterns of sunlight. Exposure causes the refractive index of fiber to rise permanently, causing a fixed index modulation following the exposure pattern. By examining the quick changes in panel temperature over time for both indoor and outdoor environments, the special powers of fiber-optic sensors are put on display. On-panel temperature effects of incident radiation flux and inclination angle are examined.

Figure.2.2 show that positions of FBG sensor on the solar panel where temperatures are measured. The chosen PV panels have dimensions of 480*720 mm and 240*360 mm, respectively. On both panels, the temperature is monitored at the three specified places O, A, and B. The next section presents the important findings

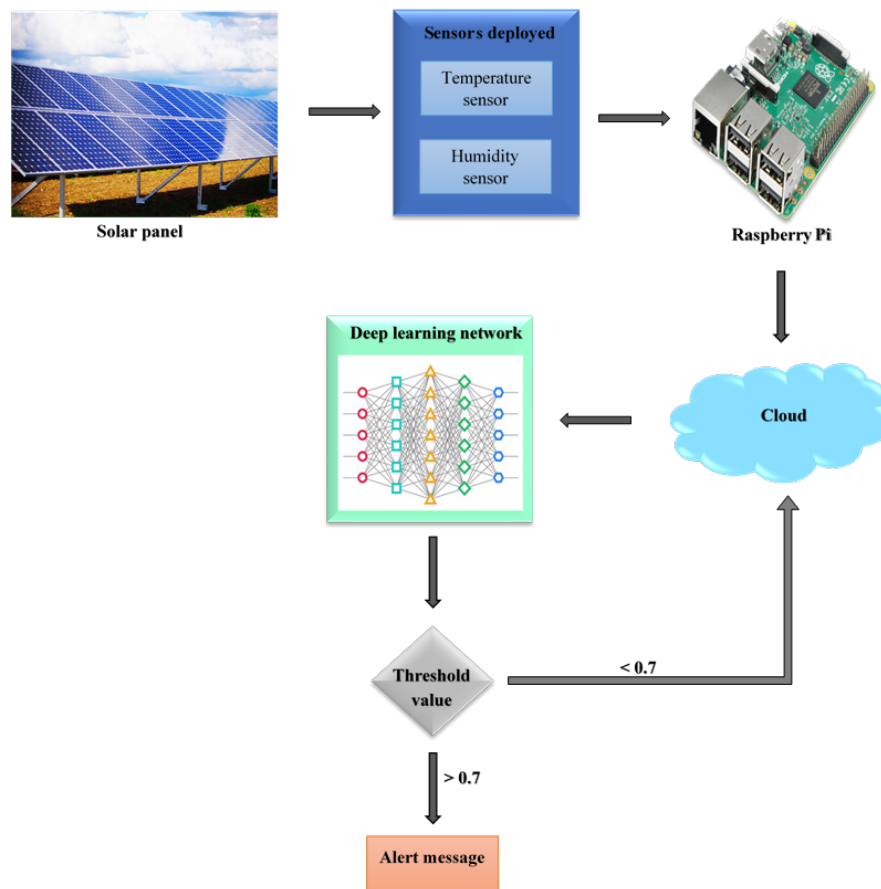


Fig. 2.1: The overall workflow of the proposed methodology

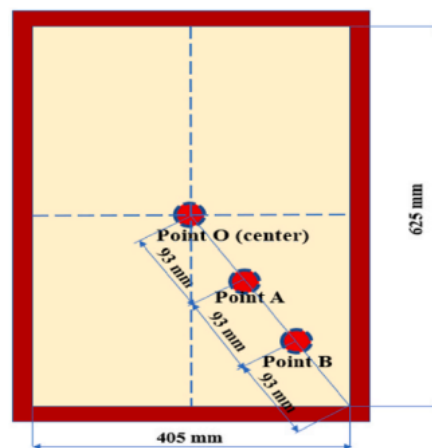


Fig. 2.2: Positions of FBG sensor on the solar panel Temperature measurements are conducted at various locations on the solar panel

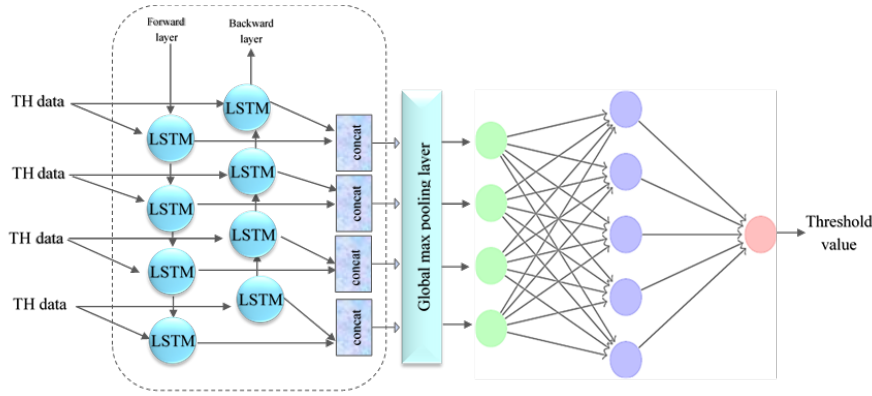


Fig. 2.3: Architecture of Bi-LSTM

from both tests. The equation states that the electrical efficiency of the PV system declines with temperature,

$$E_{eff} = E_{ref}[1 - \alpha(temp - \beta)] \quad (2.1)$$

where E_{eff} is the electrical efficiency at temperature $temp$, E_{ref} is the efficiency at reference temperature α and β is the temperature coefficient. The variations in temperature result in considerable losses in the amount of solar power produced over the long period. Additionally, running at high temperatures lowers the efficiency of solar panels and shortens their lifetime.

The Sensirion SHT15 sensor measures relative humidity with an accuracy of 2% in humidity and $0.3^{\circ}C$. The sensor must be exposed to innately aspirated air flow in order to effectively measure humidity. To measure temperature accurately, the detector must be coloured and isolated from large temperature masses and self-heating sources. This requirement was met by encasing the SHT15 in a 2-inch PV and suspending it from the underside of the node. An electrical fault was prevented by sealing the PV interface wire hole and coating it with conformal coating.

2.2. Raspberry Pi. Raspberry Pi are used as microcontrollers in this setup. A notable feature of the Raspberry Pi is its general-purpose input-output (GPIO) interface. I/O pins are used to input and output signals. This device includes an SD card slot, a Hdmi, a composite video output, a 3.5-millimeter audio outcome, a pair of USB ports, and a Wired jack. It also includes a 700 MHz ARM BCM2835 processor. The Raspberry Pi has 26 pins, 17 of which are for GPIO (general purpose input and output). Software can be used to configure these pins for starting and stopping devices. The voltage that GPIOs can deliver is only 0V or 3.3V (low or high). The sensor data readings are stored in the cloud server via raspberry pi module.

2.3. Deep learning network. In this phase, the Bi-LSTM model was trained to detect the Solar PV panel lifetime based on the gathered TH data from the deployed sensors. LSTM is one of the RNN model capable of constructing a large-scale neural network structure. As opposed to RNN, the gradient problems are avoided by LSTM by using memory efficiently. However, in bi-directional LSTM, has input flowing in both directions, either backwards or forward differentiating it from a regular LSTM. As information propagates forward, the state of the LSTM model can only be determined based on previously processed input. On the other hand, Bi-LSTM takes both past and future data into account, allowing it to handle contextual data efficiently.

There are four main parts to the LSTM classifier: memory cell, input gate, forget gate and output gate as shown in fig.3. The input data is kept in the memory cell for a short period of time or for a long period. The Input Gate controls the amount of data, whereas the Forget Gate controls information retention in the LSTM cell. By controlling the information in the LSTM layer cell, output activation for the gate can be computed and

formatted. The relationship between input, hidden states, and different gates can be derived from equations (1 to 5).

$$i_t = \sigma(\text{weight}_i * [h_{t-1}, z'_t] + \text{bias}_i) \quad (2.2)$$

$$f_t = \sigma(\text{weight}_f * [h_{t-1}, z'_t] + \text{bias}_f) \quad (2.3)$$

$$i'_t = \sigma(\text{weight}_{i'} * [h_{t-1}, z'_t] + \text{bias}_{i'}) \quad (2.4)$$

$$c_t = f_t * c_{t-1} + i_t * \tanh(\text{weight}_c * [h_{t-1}, z'_t] + \text{bias}_c) \quad (2.5)$$

$$h_t = i'_t * \tanh(c_t) \quad (2.6)$$

where i_t, i'_t, f_t and c_t represents the input gate, output gate, forget gate, and the cell at time t ; h_t and z'_t represents the hidden vectors and input vectors at time t . At the t -th time, the input z_t from the opposite is handled by the pair of parallel LSTM layers in forward and reverse directions, and the concatenate the output. LSTMs with two parallel layers operate similarly to traditional LSTM neural networks, storing information in both directions. By employing two modes of direction, Bi-LSTM retains input data from both previous and later sequences. The output series of the first LSTM is given as an input of the second LSTM, and the output series of the second LSTM layer is the concatenated to the last units of the forward and backward layers as,

$$H_{\text{output}} = \{H_{\text{forward}}, H_{\text{backward}}\} \quad (2.7)$$

The primary function of the global max pooling layer is to extract as many features as possible from the given temporal data. A Flatten layer is typically used to transform the final feature maps into a one-dimensional array. The one-dimensional array is then used as the input of the fully connected layer. The FC layer is the feed-forward neural network, and all the neurons between layers are interconnected. By multiplying the inputs by the weight matrices and adding the bias vectors, the output of the FC layer is determined as,

$$O(z) = \text{softmax}(\text{weight} * z + \text{bias}) \quad (2.8)$$

where z denotes the input of fully connected and $O(z)$ denotes the output of the network. The softmax layer translates the values into prospects, and the prediction layer gives the threshold value based the TH data. The primary device of the solar PV panel lifetime detection system is Raspberry Pi which is used to store the data collected by different sensors. These data are transferred to cloud server using Raspberry Pi. Based on the gathered data the deep learning-based Bi-LSTM network is used to detect the panel lifetime using the threshold value. Besides, if there are any changes inside the solar panel then users will be notified by SMS which is done by GSM module.

3. Results and discussions. In this section, the proposed approach is Based on the TH information from the deployed sensors, various measures such as accuracy, specificity, and sensitivity were calculated. The benchmark comprises the overall accuracy rate, which is explicitly specified and evaluated, as well as the proposed approach's performance. The proposed model's efficiency can be measured using the evaluation metrics specificity, sensitivity, and accuracy.

$$\text{Specificity} = \frac{TN}{TN + FP} \quad (3.1)$$

$$\text{Sensitivity} = \frac{TP}{TP + FN} \quad (3.2)$$

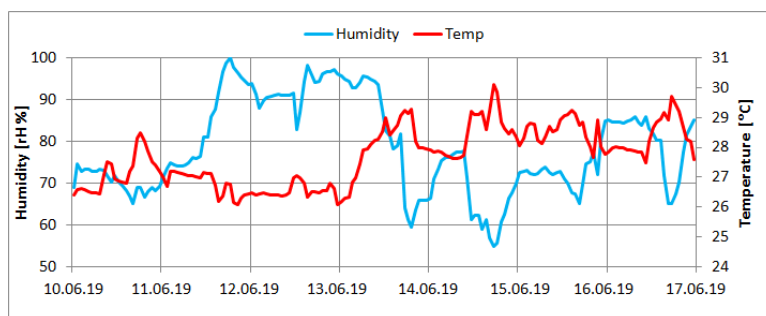


Fig. 3.1: Graphically depiction of Monthly Temperature-Humidity variation

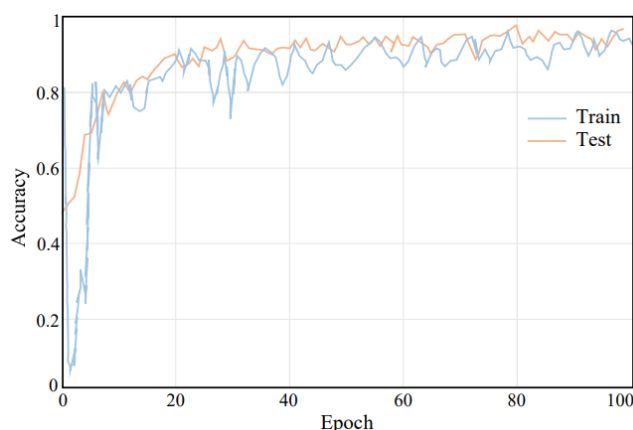


Fig. 3.2: Accuracy curve of Bi-LSTM

$$Accuracy = \frac{TP + TN}{TN + TP + FN + FP} \quad (3.3)$$

Figure 3.1 shows the monthly variation of the outdoor climatic factors. Over a one-week period, temperatures and humidity range from 25.9 to 30.2 C and 56.2 to 95.4%, respectively. The graph shows the dramatic drop in interior CO, CO₂ and NO₂ concentrations caused by Natural ventilation is achieved by opening doors and windows first thing in the morning. On 14.06.2021, CO concentration reduced from 5.24 mg.m⁻³ to 1.35 mg.m⁻³, Nitrogen oxides accumulation decreased from 61 g.m⁻³.51 to 15 g.m⁻³.1, and CO₂ concentration decreased from 420 g.m⁻³.1 to 301 g.m⁻³.1. Increased gas concentration levels in a closed and poorly ventilated environment for an extended period of time resulted in a 75% reduction in CO, 74% reduction in NO₂, and 27% reduction in CO₂ as a consequence of natural ventilation. The results reveal that household activities have a significant impact on indoor air quality. Although natural ventilation has been encouraged by the system, the outside air quality has been significantly improved by its warnings.

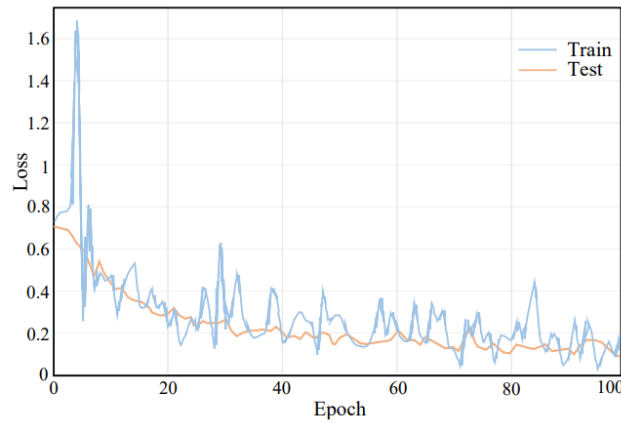


Fig. 3.3: Loss curve of Bi-LSTM

Table 3.1: Comparison between traditional networks and DRC Net

Networks	Specificity	Sensitivity	Accuracy
CNN	86.2	84.5	91.2
LSTM	85.7	84.2	93.5
Bi-LSTM	89.6	88.0	95.2

In Figure 3.2, the accuracy curve can be seen as the number of epochs on the horizontal axis and the range of accuracy on the vertical axis. As the number of epochs increases, the accuracy of the DRC net improves. Figure. displays the epoch and loss range, which shows that The disadvantage of the Bi-LSTM decreases as the epochs are increased. The proposed Bi-LSTM has a highly accurate range for identifying different cry signal classes. This study began by calculating the size of training epochs required to achieve the highest level of checking accuracy. The classification performance of Bi-LSTM was accomplished at 100 training examples by achieving the testing accuracy, according to the results of 95.2% with low error rate.

The efficiency of each Deep learning networks was estimated to show that the proposed Bi-LSTM attains high precision. A examination of the suggested Bi-LSTM with classification models like as CNN and LSTM was performed. The performance of each network was evaluated using various metrics such as specificity, sensitivity, and accuracy, as shown in table.3.1.

From table.3.1, the comparison has been performed between different approaches on basis of the specific performance parameters by attaining the best accuracy range. Moreover, the traditional networks are not achieved high accuracy compared to the Bi-LSTM. The accuracy attained by proposed method is 95.2%, which was higher than the traditional DL networks. The proposed Bi-LSTM increases the overall accuracy range by 4.20% and 1.78% better than CNN and LSTM respectively. As can be shown in Table.1, our technique is clearly superior than other methods. So, the predicted outcomes of the proposed Bi-LSTM are extremely reliable for recognizing the lifetime of the solar PV panel.

4. Conclusion. This paper focuses on introducing a Deep learning model to predict the lifetime of solar PV panel for sustaining performance and maximizing the productive life of solar panels. Initially, the temperature and humidity (TH) data are collected from the solar photovoltaic panel using the fibre-optic sensor and Sensirion SHT15 sensor. The primary device of the solar PV panel lifetime detection system is Raspberry Pi which is used to store the data collected by different sensors. These data are transferred to cloud server using Raspberry Pi. Based on the gathered data the deep learning-based Bi-LSTM network is used to detect the panel lifetime using the threshold value. Besides, if there are any changes inside the solar panel then users will be notified by SMS

which is done by GSM module. The performance of the Bi-LSTM was evaluated using the specific parameters like specificity, sensitivity and accuracy. The experimental findings reveal that the proposed approach attains a better accuracy of 95.2% for detecting the life of the solar panel. The proposed Bi-LSTM increases the overall accuracy range by 4.20% and 1.78% better than CNN and LSTM respectively. In future, the advanced transfer learning networks can be used to improve the performance in lifetime detection of the solar PV panel.

REFERENCES

- [1] S. Dhanalakshmi, P. Nandini, S. Rakshit, P. Rawat, R. Narayanamoorthi, R. Kumar, and R. Senthil, Fiber Bragg grating sensor-based temperature monitoring of solar photovoltaic panels using machine learning algorithms. *Optical Fiber Technology*, 69, p.102831. 2022.
- [2] S. Dhanalakshmi, V. Chakravartula, R. Narayanamoorthi, R. Kumar, G. Dooly, D.B. Duraibabu, and R. Senthil, Thermal management of solar photovoltaic panels using a fibre Bragg grating sensor-based temperature monitoring. *Case Studies in Thermal Engineering*, 31, p.101834. 2022.
- [3] S. Sarkar, D. Inupakutika, M. Banerjee, M. Tarhani, and M. Shadaram, Machine Learning Methods for Discriminating Strain and Temperature Effects on FBG-Based Sensors. *IEEE Photonics Technology Letters*, 33(16), pp.876-879.Ff, 2021.
- [4] S. Sarkar, D. Inupakutika, M. Banerjee, M. Tarhani, M.K. Eghbal, and M. Shadaram, Discrimination of strain and temperature effects on FBG-based sensor using machine learning. In *2020 IEEE Photonics Conference (IPC)* (pp. 1-2). IEEE. 2020
- [5] E.A. Santolin, I.D. Lourenço Junior, V.D. Corte, J.C.C.D. Silva, and V.D. Oliveira, Thermal monitoring of photovoltaic module using optical fiber sensors. *Journal of Microwaves, Optoelectronics and Electromagnetic Applications*, 15, pp.333-348, 2016.
- [6] S.N. Venkatesh, B.R. Jeyavadhanam, A.M. Sizkouhi, S.M. Esmailifar, M. Aghaei, and V. Sugumaran, Automatic detection of visual faults on photovoltaic modules using deep ensemble learning network. *Energy Reports*, 8, pp.14382-14395, 2022.
- [7] Y. Chaibi, A. Allouhi, M. Malvoni, M. Salhi, and R. Saadani, Solar irradiance and temperature influence on the photovoltaic cell equivalent-circuit models. *Solar Energy*, 188, pp.1102-1110, 2019.
- [8] M. Zaimi, H. El Achouby, A. Ibral, and E.M. Assaid, determining combined effects of solar radiation and panel junction temperature on all model-parameters to forecast peak power and photovoltaic yield of solar panel under non-standard conditions. *Solar Energy*, 191, pp.341-359. 2019.
- [9] W. Wei, H.Z. Mei, and P. Xue, Fibre Bragg Grating sensing-based temperature monitoring system of power transformer. *International Journal of Heat and Technology*, 36(3), pp.877-882. 2018.
- [10] S. Daud, M.S. Abd Aziz, K.T. Chaudhary, M. Bahadoran, and J. Ali, Sensitivity measurement of fibre Bragg grating sensor. *Jurnal Teknologi*, 78(3), 2016.
- [11] M.V. Reddy, R.S. Prasad, R.S. Srimannarayana, M. Manohar, and T.V. Apparao, December. FBG-based temperature sensor package. In *2014 9th International Conference on Industrial and Information Systems (ICIIS)* (pp. 1-4). IEEE, 2014
- [12] S. Daud, and A.F.A. Noorden, Fibre Bragg grating sensor system for temperature application. *Jurnal Teknologi*, 78(3), 2016.
- [13] M.A. Jucá, and A.B. dos Santos, Fiber Bragg grating interrogation using FBG filters and artificial neural network. In *2017 SBMO/IEEE MTT-S International Microwave and Optoelectronics Conference (IMOC)* (pp. 1-4). IEEE, 2017.
- [14] D. Tosi, Review and analysis of peak tracking techniques for fiber Bragg grating sensors. *Sensors*, 17(10), p.2368. 2017.
- [15] S.A. Kadhim, S.A.A. Taha, and D.A. Resen, Temperature Sensor Based on Fiber Bragg Grating (FBG), Implementation, Evaluation and Spectral Characterization Study. *International Journal of Innovative Research in Science, Engineering and Technology*, 4(9), pp.8038-8043, 2015.

Edited by: Bradha Madhavan

Special issue on: High-performance Computing Algorithms for Material Sciences

Received: Jul 29, 2024

Accepted: Nov 7, 2024